Hydroxylation of Camphor by Reduced Oxy-Cytochrome P450cam: Mechanistic Implications of EPR and ENDOR Studies of Catalytic Intermediates in Native and Mutant Enzymes

Roman Davydov,[†] Thomas M. Makris,[‡] Victoria Kofman, David E. Werst,[§] Stephen G. Sligar,*[,‡] and Brian M. Hoffman*[,†]

Contribution from The Department of Chemistry, Northwestern University, Evanston, Illinois 60201, The Beckman Institute, Departments of Chemistry and Biochemistry, and The Center for Biophysics, University of Illinois, Urbana Illinois 61801, and Chemistry Division, Argonne National Laboratory, Argonne, Illinois 60439

Received October 4, 2000

Abstract: We have employed γ-irradiation at cryogenic temperatures (77 K and also ~6 K) of the ternary complexes of camphor, dioxygen, and ferro-cytochrome P450cam to inject the "second" electron of the catalytic process. We have used EPR and ENDOR spectroscopies to characterize the primary product of reduction as well as subsequent states created by annealing reduced oxyP450, both the WT enzyme and the D251N and T252A mutants, at progressively higher temperatures. (i) The primary product upon reduction of oxyP450 **4** is the end-on, "H-bonded peroxo" intermediate **5A**. (ii) This converts even at cryogenic temperatures to the hydroperoxo-ferriheme species, **5B**, in a step that is sensitive to these mutations.Yields of **5B** are as high as 40%. (iii) In WT and D251N P450s, brief annealing in a narrow temperature range around 200 K causes **5B** to convert to a product state, **7A**, in which the product 5-exo-hydroxycamphor is coordinated to the ferriheme in a nonequilibrium configuration. Chemical and EPR quantitations indicate the reaction pathway involving **5**B yields 5-exo-hydroxycamphor quantitatively. Analogous (but less extensive) results are seen for the alternate substrate, adamantane. (iv) Although the T252A mutation does not interfere with the formation of **5B**, the cryoreduced oxyT252A does not yield product, which suggests that **5B** is a key intermediate at or near the branch-point that leads either to product formation or to nonproductive "uncoupling" and H_2O_2 production. The D251N mutation appears to perturb multiple stages in the catalytic cycle. (v) There is no spectroscopic evidence for the buildup of a high-valence oxyferryl/porphyrin π-cation radical intermediate, **6**. However, ENDOR spectroscopy of **7A** in H_2O and D_2O buffers shows that **7A** contains hydroxycamphor, rather than water, bound to Fe^{3+}, and that the proton removed from the C(5) carbon of substrate during hydroxylation is trapped as the hydroxyl proton. This demonstrates that hydroxylation of substrates by P450cam in fact occurs by the formation and reaction of **6**. (vi) Annealing at ≥220 K converts the initial product state **7A** to the equilibrium product state **7**, with the transition occurring via a second nonequilibrium product state, **7B**, in the D251N mutant; in states **7B** and **7** the hydroxycamphor hydroxyl proton no longer is trapped. (vii) The present results are discussed in the context of other efforts to detect intermediates in the P450 catalytic cycle.

Members of the cytochrome P450 monooxygenase family play vital roles in the synthesis and degradation of many physiologically important compounds and xenobiotics.[1] The P450 hydroxylation reaction is postulated to follow the mechanism of Scheme 1,[1,2] in which the overall rate-limiting step for hydroxylation by the native enzyme is the reduction of the dioxygen-bound ferrous state (**4**), and which contains hypothetical intermediates between species **4** and **7** whose structures have not been established.[3]

Recently, we presented[4] the first stage of an investigation of the P450 enzymatic cycle through EPR and ENDOR spectroscopic investigations of catalytically active cytochrome P450cam intermediate states[4] prepared by radiolytic cryoreduction[5−10] of **4**. These studies involve not only the wild-type (WT) enzyme, but also two site-specific mutations to the distal-pocket proton delivery system. The T252A mutant of P450cam shows an uncoupling of O_2 consumption from product formation.[11−13] The

[†] Northwestern University.
[‡] University of Illinois.
[§] Argonne National Laboratory.

(1) Ortiz de Montellano, P. R.; Correia, M. A. *Cytochrome P450*, 2nd ed.; Plenum Press: New York, 1995; Vol. 2.
(2) Benson, D. E.; Suslick, K. S.; Sligar, S. G. *Biochemistry* **1997**, *36*, 5104−5107.
(3) Sono, M.; Roach, M. P.; Coulter, E. D.; Dawson, J. H. *Chem. Rev.* **1996**, *96*, 2841−2887.
(4) Davydov, R.; Macdonald, I. D. G.; Makris, T. M.; Sligar, S. G.; Hoffman, B. M. *J. Am. Chem. Soc.* **1999**, *121*, 10654−10655.
(5) Symons, M. C. R.; Petersen, R. L. *Proc. R. Soc. London B* **1978**, *201*, 285−300.
(6) Davydov, R. M. *Biofizika* **1980**, *25*, 203−207.
(7) Kappl, R.; Höhn-Berlage, M.; Hüttermann, J.; Bartlett, N.; Symons, M. C. R. *Biochim. Biophys. Acta* **1985**, *827*, 327−343.
(8) Leibl, W.; Nitschke, W.; Hüttermann, J. *Biochim. Biophys. Acta* **1986**, *870*, 20−30.
(9) Davydov, R.; Kappl, R.; Hutterman, R.; Peterson, J. *FEBS Lett.* **1991**, *295*, 113−115.
(10) Davydov, R.; Kuprin, S.; Graslund, A.; Ehrenberg, A. *J. Am. Chem. Soc.* **1994**, *116*, 11120−11128.
(11) Martinis, S. A.; Atkins, W. M.; Stayton, P. S.; Sligar, S. G. *J. Am. Chem. Soc.* **1989**, *111*, 9252−9253.
(12) Imai, M.; Shimada, H.; Watanabe, Y.; Matsushima-Hibiya, Y.; Makino, R.; Koga, H.; Horiuchi, T.; Ishimura, Y. *Proc. Natl. Acad. Sci. U.S.A.* **1989**, *86*, 7823−7827.
(13) Raag, R.; Martinis, S. A.; Sligar, S. G.; Poulos, T. L. *Biochemistry* **1991**, *30*, 11420−11429.

10.1021/ja003583l CCC: $20.00
Published on Web 01/30/2001

Scheme 1

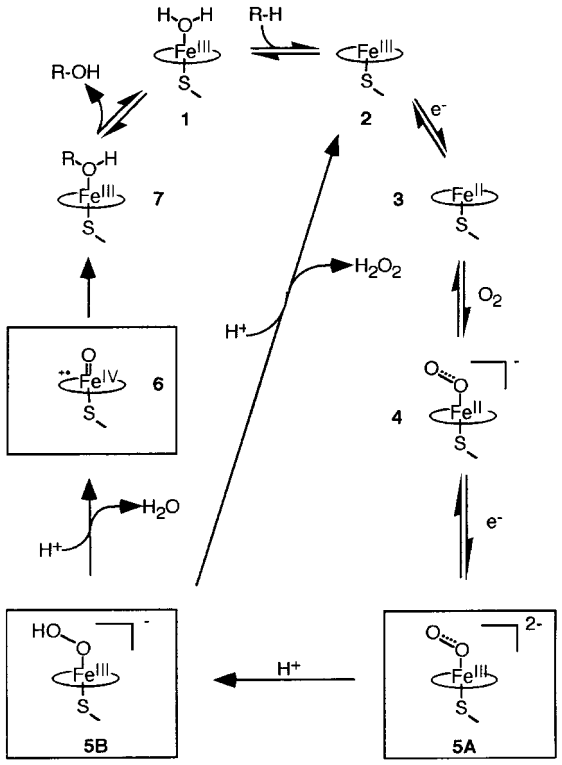

D251N mutant retains catalytic activity, but the overall rate of catalysis is drastically slowed, while the observed solvent isotope effect is dramatically increased.[14] A key result in our first report, confirmed and extended here, is that the WT and D251N mutant, which are enzymatically competent in ambient-temperature experiments, likewise produce the 5-exo-hydroxycamphor product upon annealing of the cryoreduced oxy-enzymes to higher temperatures, while the T252A mutant does not produce product under either type of condition.

The prior EPR specta *and* ^{1}H proton ENDOR results for the cryoreduced-oxyP450cam-WT and T252A mutant indicated that for both the species trapped at 77 K is the hydroperoxo-ferric-intermediate (**5B**); thus, even at this temperature the first proton of catalysis can be delivered to the heme-bound dioxygen upon reduction of **4** in these enzymes. In a separate study this was also observed for the oxygen-activating enzyme, heme oxygenase,[15] and is in contrast to the case of proteins such as Hb and Mb,[5−8] which are "designed" for carrying dioxygen, rather than activating it, and where higher-temperature annealing is needed to form the hydroperoxo species. However, it was found that the cryoreduced oxyT252A does not yield product, while the WT P450 does. From this we inferred that **5B** is a key intermediate at or near the branch-point that leads either to product formation or to "uncoupling" in which O−O bond cleavage is replaced by H_2O_2 production. As the T252A mutation did not interfere with the formation of **5B**, it appeared that this mutation perturbs the delivery of the *second* proton of catalysis. In contrast, for the D251N mutant 77 K cryoreduction of **4** led to the observation of a low-spin ferriheme EPR signal that, in accordance with prior studies of cryoreduced oxyHb and -Mb,[5−8] was provisionally assigned as a hydrogen-bonded, end-on "peroxo-ferric" species, denoted **5A**. This species converts to **5B** when transiently warmed to ∼180 K, and **5B** goes on to form product upon annealing to higher temperatures. Thus, this mutation appeared to inhibit the delivery of the *first* proton of catalysis.

To extend our observations of P450 intermediates, we have now cryoreduced samples at 77 K and taken them, stepwise, through the catalytic pathway by numerous sequential annealing steps at progressively higher temperatures, collecting extensive EPR and ENDOR data on each intermediate observed. In addition, we complement these measurements with cryoreduction experiments performed in an EPR cavity at ∼6 K. These studies characterize the stages of the catalytic cycle between species **4** and **7** of Scheme 1, as summarized below (in Scheme 2). Among other results, the present studies: establish the nature of the primary product of the one-electron reduction of **4**; indicate it to be the same species in WT and mutant enzymes; show that the reaction pathway involving **5B** yields 5-exo-hydroxycamphor quantitatively, and that there is no other pathway to product; demonstrate that catalytic hydroxylation in P450cam occurs by attack on substrate of the high-valence oxyferryl/porphyrin π-cation radical intermediate, **6**. The present results are discussed in the context of other efforts to observe intermediates in the P450 catalytic cycle.[16,17]

Materials and Methods

The preparations of P450cam[18] and mutants (T252A,[13] D251N[19]) have been described; the samples contained 1 mM protein, 0.1 M KPi (pH 8.0), 1.6 mM camphor and 15% v/v glycerol. As desired, samples were exchanged five times into D_2O buffers that contained d_3-glycerol.The equilibrium product complex of hydroxycamphor bound to ferriP450, was prepared with the WT and D251N mutant enzymes by adding exo-5-hydroxycamphor to the substrate free enzyme to a final concentration of 2 mM. Adamantane and adamantanol bound complexes were prepared by adding the methanol dissolved substrate dropwise to a final concentration of 0.2 M (methanol concentrations never exceeded 5% v/v). Substrate-free P450 was prepared by passage through a Shodex gel-filtration column (Waters) equilibrated in 50 mM Tris-HCl pH 7.4, and the resulting protein exchanged in 0.1 M KPi and 15% v/v glycerol. The oxyP450 complexes were prepared by dithionite reduction of anaerobic solutions, anaerobic chromatographic removal of dithionite, and then bubbling at 0° C with O_2 for 20 s (T252A) and 60 s (P450cam and D251N); they were then stored in quartz EPR tubes at 77 K until cryoreduction. In all but one instance, discussed shortly, the oxyP450 samples were reduced at 77 K by γ-irradiation with a ^{60}Co source to a dose of ∼3 Mrad as described,[4,15,20] and then kept at 77 K. In general, samples were examined by EPR at 77 K and 2 K within 12−24 h, then returned to 77 K storage for later annealing and EPR and ENDOR study. In no case did we observe annealing effects through storage at 77 K. Chemical determination of product yields was performed by gas chromatography. OxyD251N samples (irradiated at 77 K for various times) were extracted with 3 volumes of chloroform in the presence of *endo*-5-bromocamphor (Sigma), which served as an internal standard, and dried with magnesium sulfate under a stream of dry nitrogen. GC analysis was carried out using a cross-linked 5% methyl phenyl siloxane column with a single ramp temperature program.[2] Signals with retention times of 7.8, 11.4, and 12.3 corresponding to 1*R*-(+)-camphor, *exo*-5-hydroxycamphor, and *endo*-5-bromocamphor, were integrated and used to define product concentration. The flame ionization of reaction product and internal standard has previously been shown to be identical.

(14) Vidakovic, M.; Sligar, S. G.; Li, H.; Poulos, T. L. *Biochemistry* **1998**, *37*, 9211−9219.
(15) Davydov, R. M.; Yoshida, T.; Ikeda-Saito, M.; Hoffman, B. M. *J. Am. Chem. Soc.* **1999**, *121*, 10656−10657.
(16) Egawa, T.; Shimada, H.; Ishimura, Y. *Biochem. Biophys. Res. Commun.* **1994**, *201*, 1464−1468.
(17) Schlichting, I.; Berendzen, J.; Chu, K.; Stock, A. M.; Maves, S. A.; Benson, D. E.; Sweet, B. M.; Ringe, D.; Petsko, G. A.; Sligar, S. G. *Science* **2000**, *287*, 1615−1622.
(18) Gunsalus, I. C.; Wagner, G. C. *Methods Enzymol.* **1978**, *52*, 166−188.
(19) Gerber, N. C.; Sligar, S. G. *J. Biol. Chem.* **1994**, *269*, 4260−4266.
(20) Davydov, R.; Valentine, A. M.; Komar-Panicucci, S.; Hoffman, B. M.; Lippard, S. J. *Biochemistry* **1999**, *38*, 4188−4197.

As desired, the cryoreduced samples were annealed at temperatures above 77 K by transferring a sample from liquid nitrogen to a bath at fixed temperature for 1 min unless specified otherwise, after which the sample was transferred back to liquid nitrogen. For consistency, we quote clock times for annealing. However, examination of a thermocouple frozen in a Q-band tube (2.5 mm OD) showed that an approximate equilibrium with the bath occurred in ~15−20 s. Thus, for example, a reported 1 min annealing at temperature *T* corresponds to ~40−45 s *at* T. Each cryoreduction discussed here was repeated several times with results that are wholly compatible, but that vary slightly in the apparent degree of a particular conversion at a particular bath temperature as the result of the imprecision associated with the short annealing periods. We emphasize here the semiquantitative nature of the discussions of annealing. Finally, in many instances cryoreduction creates a major species plus one or more minority forms, representative of a distribution among conformational substates in the precursor state. If nothing is lost from an argument, we ignore minority forms.

X-band EPR spectra were recorded on a modified Varian E-4 spectrometer at 77 K. Q-band (35 GHz) EPR and ENDOR spectra were recorded on a modified Varian E-110 spectrometer equipped with a helium immersion Dewar. These spectra, which were obtained in dispersion mode using 100 kHz field modulation under "rapid passage" conditions,[21−23] have the appearance of absorption spectra; derivative presentations were generated digitally using LabCalc. For ENDOR, in some instances, the radio frequency (RF) bandwidth was broadened to 100 kHz to improve the signal-to-noise ratio.[24] EPR spectra of cryoreduced samples exhibit strong signals from free radicals created by the irradiation; this region is deleted from the spectra shown. The EPR signals of the cryoreduced oxyP450 and of the product complex forming after annealing were quantitated using a 1mM solution of the low-spin ferricytochrome P450-hydroxycamphor complex as a standard.

A single WT oxyP450 sample was cryoreduced at $T \approx 6$ K by irradiation with a 3 MeV electron beam from a Van de Graaff accelerator while held in the helium-flow cryostat of a Bruker 200-series X-band EPR spectrometer. During irradiation the EPR cavity was translated vertically to allow only the cryostat and sample to be exposed to the electron beam. The electron beam was operated in the pulsed mode (approximately 2 krad per pulse) and low repetition rate (1−2 Hz). Cumulative doses used were in the range 1−3 Mrad. The most serious interference from radiation-induced EPR signals in the cryostat Dewar and sample cell in the spectral range of interest to this study were the trapped hydrogen atoms. These signals are broadened because they, in part, arise from three concentric fused silica tubes, each experiencing a slightly different magnetic field, along with broadening by passage effects for these H atoms and those produced in the sample.

For a single orientation of a paramagnetic center, the first-order ENDOR spectrum of a nucleus with $I = {}^1/_2$ in a single paramagnetic center consists of a doublet with frequencies given by:[25]

$$\nu_{\pm} = |\nu_N \pm A/2| \quad (1)$$

Here, ν_N is the nuclear Larmor frequency and A is the orientation-dependent hyperfine coupling constant of the coupled nucleus. The doublet is centered at the Larmor frequency and separated by A when $\nu_N > |A/2|$, as is the case for ^{1}H spectra presented here. For 14N ($I = 1$), a single orientation gives a four-line pattern

$$\nu_{\pm}(\pm) = |\nu_N \pm A/2 \pm 3P/2| \quad (1a)$$

in which both the ν_+ and ν_- branches described by eq 1 are further split into two lines by the quadrupole splitting, 3P. For heme pyrrole ^{14}N studied here, only the $\nu_{\pm}(\pm)$ branch is readily observed in spectra collected at 35 GHz. The full hyperfine and quadrupole tensors of a coupled nucleus can be obtained by analyzing a "2-D" field-frequency set of orientation-selective ENDOR spectra collected across the EPR envelope, as described elsewhere.[26,27]

Table 1. *g*-Values for Equilibrium Low-Spin Forms of P450cam and for Intermediates Formed during the Hydroxylation of Camphor

equilibrium forms	*g*-values g_1	g_2	g_3
aquoferriP450[a] **1**	2.450	2.26	1.910
aquoferriP450 + cam[a,b] **2**	2.410	2.24	1.961
ferriP450 + camOH[c] **7**	2.486	2.25	1.90[a]
+ adamantanol[d]	2.5	2.298	1.89
enzymatic intermediates			
5A	2.246	~2.166	~1.958 (minor)
WT **5B**	2.290	2.166	1.958
7A	2.620	2.180	1.865
5A	2.250	2.163	1.956
	2.224	2.150	~1.956 (minor)
5B	2.290	2.170	1.956
D251N **7A**	2.620	2.180	1.865
7B	2.510	2.250	1.890
7	2.480	2.250	1.900
T252A **5B**	2.306	2.165	~1.956

[a] Lipscomb, 1980.[29] [b] Majority species for **2** is high spin, with $g =$ [7.75, 3.97, 1.90]. [c] Spectra are indistinguishable for WT[29] and D251N. [d] Average values for a distribution of conformers.

Results

EPR of Equilibrium P450 States. Resting state, ferric P450 (**1**) exists as a low-spin aquoferriheme [28,29] form showing a single rhombic EPR signal with *g*-values of 2.45, 2.26, and 1.91 (Table 1). The reactant complex of ferric cytochrome P450cam + camphor (**2**) shows a high-spin EPR signal (major fraction), a new low-spin EPR signal, as well as a signal like that of (**1**); the *g*-values are given in Table 1.[29] The product complex (**7**), prepared by adding hydroxycamphor to ferric P450cam, shows a rhombic low-spin EPR signal with *g*-values of 2.486, 2.25, and 1.90 (Table 1).[29] The EPR spectrum of the adamantanol complex indicates the presence of a distribution of conformers with slightly different *g*-values; the average tensor values are listed in Table 1. The ferrous enzyme (**3**) prepared by 1-electron reduction of the ferric form is not EPR visible; binding of dioxygen produces the oxyP450 complex (**4**), which is diamagnetic.

EPR of Cryoreduced oxyP450. Earlier we presented the 2 K Q-band EPR spectra[4] obtained after 77 K cryoreduction of the dioxygen complexes of P450cam-WT[9,30] and the two P450cam mutants, T252A and D251N; **g** tensors for these species are presented in Table 1. The spectrum of reduced-oxyP450, D251N, labeled g_1-2.25 for its g_1 component, is very similar to that of reduced-oxyMb, whereas the spectra of reduced-oxyP450−WT and T252A are themselves very similar, henceforth denoted as g_1-2.3 spectra for their g_1 component, but are distinct from that of D251N, as reported earlier.[4] The g_1-2.3 spectra for both the WT and T252A enzymes do not change upon annealing to 180 K, but the g_1-2.25 spectrum for the reduced-oxyD251N mutant largely converts to a g_1-2.3

(21) Werst, M. M.; Davoust, C. E.; Hoffman, B. M. *J. Am. Chem. Soc.* **1991**, *113*, 1533−1538.
(22) Mailer, C.; Taylor, C. P. S. *Biochim. Biophys. Acta* **1973**, *322*, 195−203.
(23) Feher, G. *Phys. Rev.* **1959**, *114*, 1219−1244.
(24) Hoffman, B. M.; DeRose, V. J.; Ong, J. L.; Davoust, C. E. *J. Magn. Res.* **1994**, *110*, 52−57.
(25) Abragam, A.; Bleaney, B. *Electron Paramagnetic Resonance of Transition Metal Ions*, 2nd ed.; Clarendon Press: Oxford, 1970.
(26) Hoffman, B. M. *Acc. Chem. Res.* **1991**, *24*, 164−170.
(27) Hoffman, B. M.; DeRose, V. J.; Doan, P. E.; Gurbiel, R. J.; Houseman, A. L. P.; Telser, J. In *Biological Magnetic Resonance*; Berliner, L. J., Reuben, J., Eds.; Plenum Press: New York and London, 1993; Vol. 13, pp 151−218.
(28) LoBrutto, R.; Scholes, C. P.; Wagner, G. C.; Gunsalus, I. C.; Debrunner, P. G. *J. Am. Chem. Soc.* **1980**, *102*, 1167−1170.
(29) Lipscomb, J. D. *Biochemistry* **1980**, *19*, 3590−3599.
(30) Nyman, P. D.; Debrunner, P. G. *J. Inorg. Biochem.* **1991**, *30*, 346.

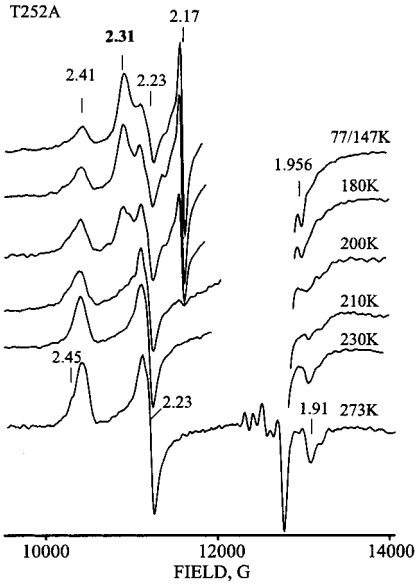

Figure 1. EPR spectra of the ternary complex of camphor, dioxygen, and T252A mutant ferro P450cam reduced radiolytically at 77 K. Spectra taken after annealing at the indicated temperatures for 1 min. Free radicals signals around $g = 2$ are omitted for clarity. *Conditions:* 35.1 GHz; $T = 2$K, 100 kHz field modulation, modulation amplitude 4 G.

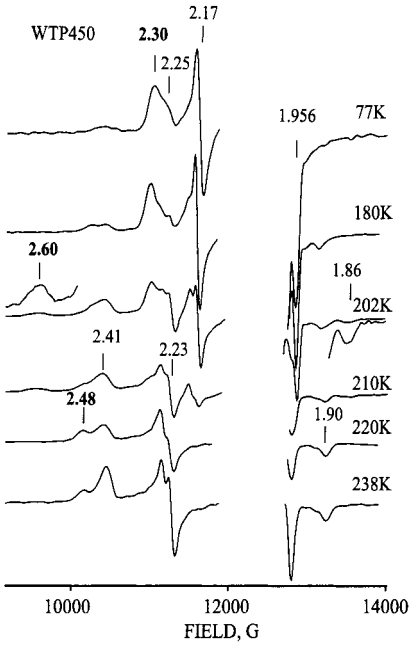

Figure 2. EPR spectra of the ternary complex of camphor, dioxygen, and WT ferro P450cam reduced radiolytically at 77 K after annealing at the indicated temperatures for 1 min. Free radicals signals around $g = 2$ are omitted for clarity. *Conditions:* as in Figure 1 except, 35.2 GHz.

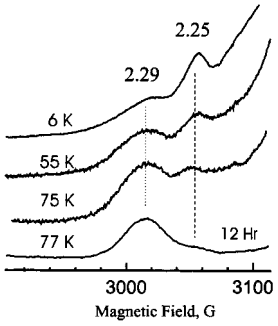

Figure 3. X-band EPR spectra of WT oxyP450 reduced radiolytically at 6 K and after annealing at the indicated temperatures for 5 min in the EPR cavity and re-cooling. Final spectrum was taken at 77 K after annealing for 12 h at this temperature. *Conditions:* $T = 6$K, 100 kHz, modulation amplitude 5 G, MW frequency 9.61 Ghz, MW power 0.1 mW, except for last spectrum where, $T = 77$ K, modulation amplitude 5 G, MW power 10 mW.

spectrum upon such treatment. All these spectra have the unmistakable signature of a low-spin ferriheme species, ($g_1 > g_2 > g_e > g_3$) in a strong ligand field (small g dispersion).[31,32]

In analogy to the assignment made for the primary products of cryoreduction in Mb and Hb,[5,7] we provisionally assigned the g_1-2.25 species as the primary "ferric-peroxo" complex, **5A**.[4] The g_1-2.3 reduced oxyheme complex is provisionally assigned to the hydroperoxyferri-protein, **5B**, created when **5A** abstracts a proton from within the heme pocket. This assignment is supported by observation that the spectra for the cryoreduced-oxyP450-WT and T252A are essentially the same as for hydroperoxo-ferriMb and Hb [5−8], and have similar **g** tensors, most particularly g_1, to those for *n*- and *tert*-butylperoxo-ferriheme-thiolate model compounds: $g \approx [2.29, 2.21, 1.96]$.[33]

To check if variation in the substrate has an effect on the electronic structure of the catalytic P450 intermediates we performed analogous cryoreduction experiments with the complex of adamantane and oxyP450 D251N. P450cam is known to catalyze hydroxylation of adamantane to adamantanol.[1] The EPR spectrum of the cryoreduced adamantane complex of oxyP450 D251N + adamantane is the same as that of **5A** for the cryoreduced oxyP450 D251N + camphor (Table 1; Figure S1). Thus, replacement of camphor by adamantane does not detectably influence the structure of the reduced oxyheme.

Annealing Measurements. Cryoreduced samples were progressively annealed in numerous small steps, as described in Materials and Methods, and examined by EPR after each step. Figures S1−S3 in Supporting Information present, respectively, the spectra from every annealing step for the T252A, WT, and D251N P450s. Figures 1−3 present corresponding subsets of the most illustrative spectra. In most instances in the following discussion we shall not refer specifically to the Supporting Information figures when discussing spectra not presented in the journal figures.

T252A. The simplest results were obtained with this mutant, and thus we discuss it first. Figure 1 presents the EPR spectrum of the oxyT252A mutant reduced at 77 K. It is a superposition of the spectrum of the camphor-bound aquoferri P450 (2, Table 1) and the cryoreduced, g_1-2.3, "hydroperoxo" form, **5B**. The former results from partial autoxidation of the oxycomplex during preparation; signals from the accompanying high-spin (hs) ferriheme resting-state form (Table 1) are observed at lower fields (not shown). Annealing this sample for 1 min at 147 K and then 180 K caused no change in spectra taken subsequently at either 77 K and 2 K. However, annealing for 1 min at 200 K caused a ∼50% loss of the **5B** signal, and another 1 min at 210 K completed its conversion to that of the ferriheme low-spin (ls) and high-spin (hs) forms, although the ls form in particular showed broadened lines, Figure 1. Further annealing to 230 K sharpens the signals. No further changes were caused by warming to room temperature and refreezing. These results show that the g_1-2.3 intermediate **5B** reverts directly to the ferriheme state **2** without detectable intermediates and without spectroscopic evidence of product formation. The absence of product also was demonstrated by gas chromatography (see below),[4]

(31) Taylor, C. P. S. *Biochim. Biophys. Acta* **1977**, *491*, 137−149.
(32) McGarvey, B. R. *Coord. Chem. Rev.* **1998**, *170*, 75−92.

and is consistent with the original studies carried out at ambient temperatures.[11,12]

WT. As with the T252A mutant, when the oxyWT enzyme is cryoreduced at 77 K its EPR spectrum (the 77 K spectrum in Figure 2) is dominated by the signal from the intermediate, **5B**. In this case autoxidation is less, and there is only a minor contribution from low-spin ferric P450, Figure 2. [34] However, the g_1-2.29 feature from **5B** of the sample irradiated at 77 K has a shoulder to its high-field side that, in part, arises from the g_2 feature of the spectrum of **2**, but in part appears to arise from the g_1 peak of a species with $g_1 \approx 2.25$. This feature disappears upon progressive annealing the sample first to 147 K and then to 180 K (Figure 2). As noted above (and discussed in more detail below), 77 K reduction of the oxyD251N mutant in fact gives a g_1-2.25 intermediate, **5A**, which only converts to **5B** form at temperatures above 77 K. Could the shoulder seen for the WT sample reflect a contribution from a species **5A**, which might be the true primary product of reduction?

To determine the primary product of cryoreduction, we reduced oxyP450 WT at ~6 K in situ in the EPR cavity by irradiation with 3 MeV electrons. As shown in the Figure 3, such an experiment yields a spectrum dominated by the g_1-2.25 feature of species **5A**, with only a shoulder at $g_1 \approx 2.29$. [35] As the sample temperature is raised in situ, Figure 3 shows that substantial conversion from **5A** to **5B** occurs by ~55 K and the latter is the dominant but not exclusive form at ~75 K, in agreement with the results from cryoreduction at 77 K, Figure 2. Overnight storage at 77 K almost completely converts **5A** to **5B** (Figure 3), as in the case of cryoreduction at 77 K (Figure 2).

We infer that the primary product upon reduction of WT oxyP450 is the g_1-2.25 species, **5A**. This state is stable at ~6 K, although it appears that even at this temperature the $g_1 \approx$ 2.29 hydroperoxo complex, **5B** is seen as a minor form. The $g_1 \approx 2.25$ species converts largely, but not completely, to **5B** by 77 K, and does so completely at temperatures near to ~147 K.

Returning to the annealing of the 77 K cryoreduced sample, subsequent 1-min warming of the hydroperoxo intermediate, **5B**, to 200 K causes a substantial decrease in its signal and an increase in the aquo-ferriheme $g \approx 2.4$ signal from **2**. While these observations are similar to results for the T252A mutant, unlike the case of this mutant, for WT P450 the loss of **5B** is acompanied by the appearance of two new low-spin ferriheme species. One is best seen as a weak feature at $g_1 \approx 2.6$ ($g =$ [2.62, 2.18, 1,86]), the other as a shoulder at $g_1 \approx 2.48$ ($g =$ [2.48, 2.25, 1.89]); there is also an increase in the hs signal of **2**. Upon subsequent annealing for 1 min at 210 K, **5B** disappears, as does the g_1-2.62 intermediate, while the intensity of the $g_1 \sim \approx 2.48$ signal increases. This latter signal was shown by Lipscomb in 1980[29] to arise from the product complex (Table 1) and is denoted **7**. Warming to 210 K sharpens the signals from the product-bound state, **7**. *In short, the hydroperoxo-ferric g_1-2.3 species. **5B**, converts to well-defined product states during 1−2 min at 200−210 K after first generating a new low-spin, g_1-2.6 intermediate.* At the same time there is also an increase in the hs signal from substrate-bound ferri P450.

This loss of **5B** to form first the g_1-2.6 species and then the known product state **7** is not accompanied by any signal yet

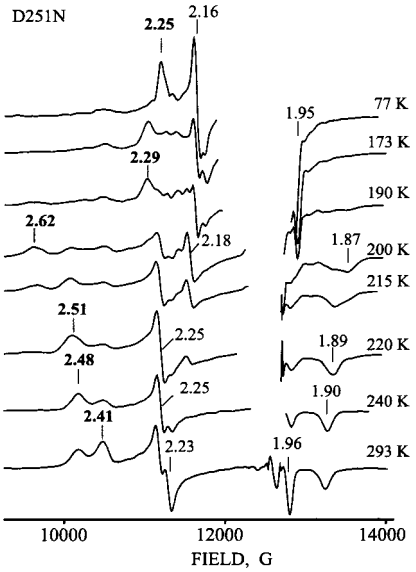

Figure 4. EPR spectra of the ternary complex of camphor, dioxygen, and D251N mutant ferro P450cam reduced radiolytically at 77 K after annealing at the indicated temperatures for 1 min. *Conditions:* as in Figure 2.

detected that can be attributed to the putative Compound I intermediate, **6**. Such a species, which contains an oxyferryl ($S = 1$) moiety spin-coupled to a cation radical, has been observed in horseradish peroxidases and numerous model compounds.[36] The g_1-2.6 signal cannot be assigned to such a species, which in general shows a roughly axial **g** tensor with $g_{\|} \approx 2$ and $g_{\perp}$ greatly different from g_e with $g_{\perp} > 2$ for ferromagnetic coupling and $g_{\perp} < 2$ for antiferromagnetic coupling. The most plausible "model" for P450 Compound I would be CPO-I because CPO also has the cysteinyl axial ligand. For CPO-I, $g =$ [2.0, 1.73, 1.64], reflective of antiferromagnetic coupling.[37] In contrast, catalase shows ferromagnetic coupling and $g =$ [3.3, 3.3, 2]. (As discussed below, a recently described intermediate with narrow *g* spread seen in the reaction of substrate-free oxyP450cam with peroxy acetic acid[38] is not a Compound I.) From these considerations, we assign the g_1-2.62 signal to a nonequilibrium product state denoted *7A*; ENDOR measurements described below confirm this assignment.

One goal of the present work was to search for the signal from intermediate **6**. Such species are most reliably detected at temperatures below 4 K under conditions of adiabatic passage,[39] precisely those employed here. However, broad scans to the limit of our magnet (~1.6 T) failed to disclose such a signal.

D251N. Unlike the oxyT252A mutant and oxyP450 WT, cryoreduction of the D251N mutant even at the "elevated" temperature of 77 K cleanly gives as the primary reduction product the *g*-2.25 intermediate, **5A**, Figure 4, with no more than ~10% conversion to **5B**. One-minute annealing steps at 139, 145, 161, and ~180 K progressively cause the loss of **5A** and a buildup of **5B**; by 161 K the spectra show the appearance of 2 ($g_1 \approx 2.4$), plus a weak feature with $g_1 \approx 2.45$ presumably from **2**. Immediately below we show that **2** does not arise in any appreciable way from **5A**, and so in general do not comment further on it. By 190 K the g_1-2.3 component of **5B** has

(33) Tajima, K.; Edo, T.; Ishizu, K.; Imaoka, S.; Funae, Y.; Oka, S.; Sakurai, H. *Biochem. Biophys. Res. Comm.* **1993**, *191*, 157−164.

(34) In addition, there is a contribution from the hs-ferriheme state (not shown).

(35) The the quality of the 6 K spectrum is diminished by the underlying tail from the $m = {}^1/_2$ H-atom line that causes the rise in intensity with increasing field. (See Materials and Methods.)

(36) Dunford, H. B. *Heme peroxidases*; John Wiley: New York, 1999.

(37) Rutter, R.; Hager, L. P.; Dhonau, H.; Hendrich, M.; Valentine, M.; Debrunner, P. *Biochemistry* **1984**, *23*, 6809−6816.

(38) Schunemann, V.; Jung, C.; Trautwein, A. X.; Mandon, D.; Weiss, R. *FEBS Lett.* **2000**, *479*, 149−154.

(39) Schulz, C. E.; Devaney, P. W.; Winkler, H.; Debrunner, P. G.; Doan, N.; Chiang, R.; Rutter, R.; Hager, L. P. *FEBS Lett.* **1979**, *103*, 102−105.

sharpened and reaches its maximum intensity. The $g_1 = 2.62$ intermediate, **7A**, appears upon annealing at 190 K, with an intensity that is no less than the maximum seen for WT enzyme. Subsequent annealing at 200 K causes the conversion of **5B** to **7A**; the loss of **5B** is completed by 1 min annealing at 210 K, a step that maximizes the intensity of **7A** at a level substantially greater than that for WT. These spectra allow complete resolution of the **g** tensor for **7A**, Table 1.

Continued progressive annealing for 1 min intervals at closely spaced temperatures (200, 210, 215, 220 K) converts **7A** to a second intermediate with $g_1 = 2.51$ (Table 1). The **7A** signal essentially disappears after a minute at 220 K, while the g_1-2.51 intermediate becomes the dominant form. The residual hs signal seen after cryoreduction (not shown) is essentially unchanged by these annealing steps. Additional warming to 240 K permits a slight reorganization of the heme environment such that the g_1-2.51 signal converts to that of the product complex, **7**, with g_1-2.48. Thawing the sample at 293 K and refreezing reequilibrates the enzyme with substrate in solution, such that final spectrum contains the well-defined signal from **7**, and that from **2** (not shown). Given this, the g_1- 2.51 species can be assigned as a second nonequilibrium ferri P450 product complex, denoted as g_1-2.5, **7B**, that is formed from the primary product complex, **7A**.

The signal from hs heme does not begin to increase until the annealing steps at 220 and 240 K; it more than doubles upon the reequilibration with substrate in solution at 293 K. Once again, spectra taken with the full field range of our magnet, ~1.6 T, showed no signal attributable to a high-valent intermediate, **6**, at any stage of the process.

Quantitation of Product Formation. Spin quantitation of the g_1-2.25 EPR signal of cryoreduced oxyD251N P450, using the ferricP450 + hydroxycamphor complex as a standard, showed that a maximum cryoreduction yield of **5B** of 0.4(1) mM out of the total ~0.9 mM oxyP450. Quantitation of the g_1-2.48 EPR signal of the product complex **7** formed in this sample by annealing at 240 K, a temperature corresponding to the maximum yield of bound product, gives 0.45(1) mM as the product yield. *We thus infer that **5A** prepared by cryoreduction of oxyD251N quantitatively converts camphor to the hydroxycamphor product.* In the WT enzyme, conversion of **5B** to the product state also is essentially quantitative, but the yield of **5B** is roughly $^1/_2$ that for D251N. The amounts of hs P450 formed upon thawing correspond roughly to what is expected for autoxidation of the nonreduced oxyP450.

In parallel we examined the dose−response of product formation as determined by GC quantitation of the stereospecifically hydroxylated 5-exo-hydroxycamphor. As shown in Figure 5, the formation of product from P450 D251N is linear in dose, with the maximum product yield of ~30%, quite compatible with the EPR results.

The implication of these EPR and chemical quantitations is that the conversion of the camphor in **5B** to stereospecifically hydroxylated hydroxycamphor is essentially quantitative.

Effect of D_2O Exchange on Annealing Cryoreduced oxyD251N. Exchange of H_2O for D_2O does not change the EPR properties of the **5A**, **7A**, or **7B** intermediates observed after cryoreduction, although the g_1 feature of **5B** showed slight broadening, Figure S4. Deuterium exchange does appear to affect the reactivities of these intermediates as observed during annealing. First, we found a ~2−3-fold decrease of the yield of the primary reduction product, **5A**, in D_2O. We further found that the conversion of **5A** to **5B** occurs at lower temperatures during annealing of D_2O samples, contrary to expectation if the rate-limiting step in this conversion involves proton transfer. Equally surprising, the g_1-2.62 primary product state, **7A**, appears to be more stable in D_2O. At 220 K, $t_{1/2}$ for the decay of **7A** in D_2O and H_2O are 6(2) min and 2(1) min, respectively.

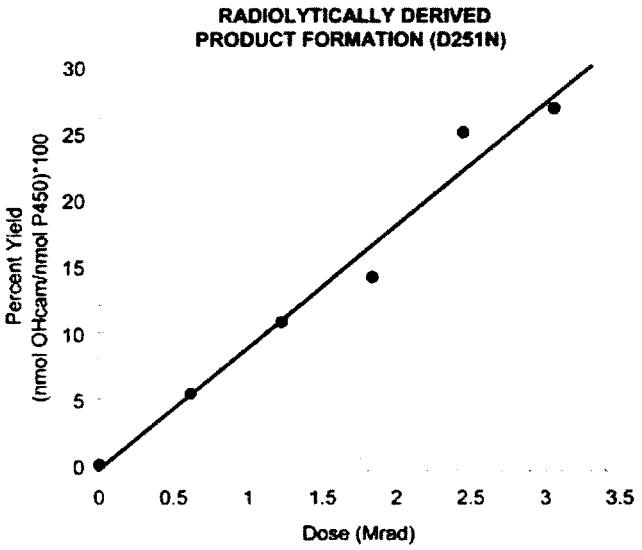

Figure 5. Dose-dependence of 5-exo-hydroxycamphor synthesis by cryoreduced oxycytochrome D251N P450cam, Plot shows dose of γ-irradiation vs yield of 5-exo-hydroxycamphor as determined by GLC (see Materials and Methods).

oxyD251N P450 + Adamantane. As with camphor, annealing cryoreduced oxyD251N P450 + adamantane at 145 K and then at 160 K results in loss of the g_1-2.25 species, **5A**, and buildup of the g_1-2.29 intermediate, **5B**. Continued progressive annealing of the sample at temperatures 182, 195, 204, and 216 K does not reveal the $g_1 = 2.6$ signal observed with the camphor-bound protein. The EPR spectrum of the sample annealed at 250 K showed a weak EPR signal from the product complex (Table 1), accounting for not more than 30% of the primary species **5A**.

^{14}N Endor Studies of P450 Intermediates. ENDOR examination of the pyrrole ^{14}N was undertaken to better characterize the catalytic P450 intermediates. The hyperfine coupling to a ^{14}N pyrrole ligand, which is roughly isotropic, provides a good measure of the spin density on Fe. In addition, the principal values of the pyrrole ^{14}N quadrupole tensor are well-known: $3\mathbf{P} \approx [-1.0, 3.2, -2.2]$, with the first value corresponding to the normal to the heme plane, the third to the Fe−N bond, and the second to the in-plane direction perpendicular to the plane of the first two.[40,41] Thus, determination of the orientation of **P** relative to the **g** tensor frame discloses the orientation of **g** relative to the molecular axes, as shown earlier.[42]

As reference, we recall that the aquo-ferriheme resting state of P450, 1, exhibits resonances from two distinct types of similar, but distinguishable pyrrole nitrogens, with an average hyperfine coupling constants along g_1 of $A_1 = 5.7$ MHz and quadrupole splitting of $|3P_1| \approx 0.9$ MHz; the inequivalence is a sign of deviations from 4-fold symmety of the heme caused by porphyrin deformations and nonsymmetrical axial interactions.[43] The observation of such sharp spectra with this small value of $3P_1$ indicates that g_1 lies essentially along the heme

(40) Brown, T. G.; Hoffman, B. M. *Mol. Phys.* **1980**, *39*, 1073−1109.
(41) Scholes, C. P.; Lapidot, A.; Mascarenhas, R.; Inubushi, T.; Isaacson, R. A.; Feher, G. *J. Am. Chem. Soc.* **1982**, *104*, 2724−2735.
(42) Lee, H.-I.; Dexter, A. F.; Fann, Y.-C.; Lakner, F. J.; Hager, L. P.; Hoffman, B. M. *J. Am. Chem. Soc.* **1997**, *119*, 4059−4069.
(43) Fann, Y.-C.; Gerber, N. C.; Osmulski, P. A.; Hager, L. P.; Sligar, S. G.; Hoffman, B. M. *J. Am. Chem. Soc.* **1994**, *116*, 5989−5990.

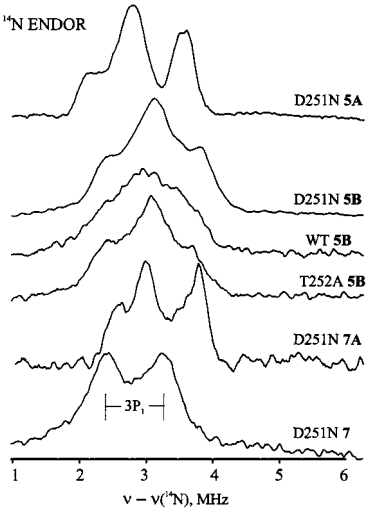

Figure 6. ^{14}N ENDOR spectra, plotted as as $[\nu - \nu_N]$ where ν_N is the Larmor frequency, taken at the g_1 field for cryoreduced oxy P450 intermediates **5A** (D251N), **5B** (D251N, WT, and T252A), **7A** (D251N), and for the equilibrium hydroxycamphor complex **7** (D251N). *Conditions:* Microwave $T = 2$ K, field modulation 100 kHz, modulation amplitude 5 G, scan speed 0.5 MHz/s, 100 kHz broadening of RF excitation.

normal, in agreement with prior single-crystal EPR measurements,[44] and thus the single-crystal-like g_1 ENDOR spectra arise from those molecules with the external field lying along the heme normal. As a measure of how protein-induced perturbations can alter the spin-Hamiltonian parameters, aquomet-CPO, which shares the same metal coordination environment of **1**, showed distinct resonances from all four pyrrole nitrogens, with average values of $A_1 \approx 6.1$ MHz and $|3P_1| \approx 1.0$ MHz.[43]

Figure 6 shows the $\nu_+(\pm)$ branch (eq 1a) of the 35 Ghz CW ^{14}N ENDOR spectra taken at g_1 for the P450 intermediates. The spectra for the different intermediates are characterized by different values of ν_N associated with different values of g_1. To eliminate the resulting shift in frequency, we plot the spectra as $[\nu - \nu_N]$, which causes the $\nu_+(\pm)$ branch for each magnetically distinct nitrogen to be centered at its value of $A/2$, and split by its value of $3P$:

$$\nu_+(\pm) - \nu_N = |A/2 \pm 3P/2| \qquad (1b)$$

One can see that in all cases the pattern center falls in the vicinity 2.9 MHz, corresponding to the average value at g_1 of, $A_1 \approx 5.8-5.9$ MHz, essentially the same as that for resting-state aquoferriP450, 1. The simple doublet pattern for **7** indicates that all 4 pyrrole ^{14}N are equivalent, with $|3P_1| \sim 0.9$ MHz. The patterns for **5A**, **5B**, and **7A** all indicate the presence of two distinct types of N with slightly different values of A, but with both having $3P_1 \approx 0.9$ MHz. This common value for $3P_1$ corresponds to the principle value of the quadrupole tensor that lies normal to the heme, and thus confirms that in all cases the g_1 axis lies normal to the heme plane, as in **1**.

Preliminary examination of spectra taken at other fields, insofar as this is possible for the various species, support the conclusion that the hyperfine tensors are primarily isotropic and that g_1 lies along the heme normal. As the hyperfine couplings in all cases are typical for a well-defined ferriheme, as exemplified by **1**,[28,43] this indicates that all the intermediates, in particular **5A** and **5B**, are to be described as rather normal ferriheme states from the viewpoint of the Fe, and have comparable spin density on the Fe(III). Interestingly, they suggest that the g_2, g_3 axes do not have the same orientation relative to the heme plane in all species, demonstrating the different distal axial ligands influence the orientation as well as the precise principal values of the **g** tensor, but these details are beyond the scope of this report.

(44) Murray, R. I.; Fisher, M. T.; Debrunner, P. G.; Sligar, S. G. In *Metalloproteins. Part 1: Metal Proteins with Redox Roles*; Harrison, P. M., Ed.; Verlag Chemie: Florida-Basel, 1985; pp 157−206.

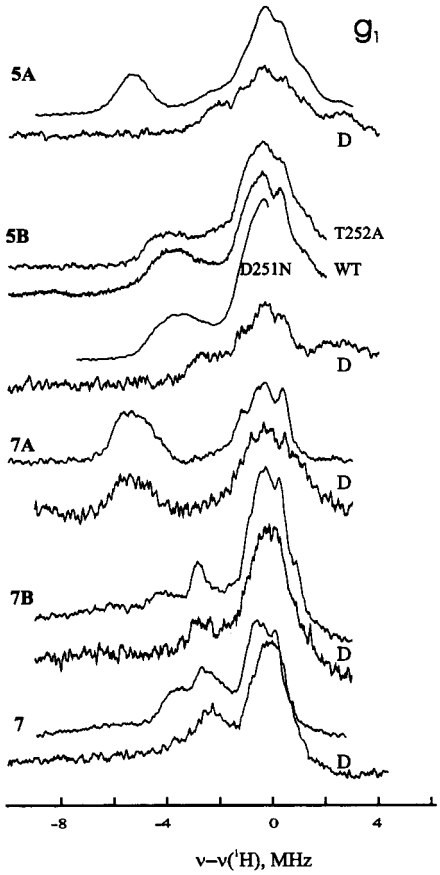

Figure 7. ^{1}H CW ENDOR spectra taken at the g_1 field for P450 reaction intermediates **5A**, **5B**, **7A**, and **7** (see text). "D" denoted prepared in D_2O buffer. If P450 variant is not denoted it is the D251N mutant. *Conditions:* 35.2 GHz, $T = 2$ K, field modulation 100 kHz, modulation amplitude 4 G, scan speed 0.5 MHz/s, 30 scans, 100 kHz broadening of RF excitation.

^{1}H ENDOR Studies of P450 Reaction Intermediates. We have employed 35 GHz ^{1}H ENDOR spectroscopy to characterize the intermediates in P450 catalysis in detail, and describe their properties sequentially, as they appear upon annealing.

Species 5. We earlier showed that the ENDOR spectra taken at g_1 for the g_1-2.25 signals of 77 K cryoreduced oxyMb, oxyHb, and oxyP450 D251N (state **5A**), and at g_1 for the g_1-2.3 signals of hydroperoxo-Hb, oxyheme oxygenase, oxyP450 WT and the T252A mutant (state **5B)** each shows a signal from a strongly coupled exchangeable proton; this is shown in Figure 7 for the P450 intermediates. The spectra are doublets, symmetric in frequency about ν_H according to eq 1; a commonly occurring asymmetry in *intensities* renders the ν_+ branch not only redundant according to the equation, but less useful for measurements, and the figure presents only the ν_- branch of each spectrum. In addition, the spectra show an intense, poorly resolved ^{1}H signal that is centered at the proton Larmor frequency, is of ∼4−5 MHz in breadth, and is largely, but not completely, nonexchangeable.

The exchangeable proton seen in the spectrum of the g_1-2.25 species in cryoreduced oxyMb in H_2O ($A(g_1) \approx 14$ MHz) had

been assigned to a hydrogen bond between the distal histidine and the "peroxo" moiety of a peroxo-ferriheme,[7] and we have provisionally adopted that assignment for **5A** seen in 77 K cryoreduced oxyP450 D251N (Figure 4). The hydroperoxo-ferric-Mb,[4] Hb,[15] and heme oxygenase[15] states each gives a signal from the exchangeable proton with a significant, although smaller, hyperfine coupling ($A(g_1) \approx 8.2$ MHz), and the same is true for the hydroperoxoferri-P450 states **5B** of P450 WT and the two mutants (Figure 4). The decrease in coupling, despite the putative change from H-bond to covalent bond upon conversion of **5A** to **5B**, might reflect a decreased spin density on the terminal oxygen of the hydroperoxy moiety compared to that on the "peroxo" one. The ^{14}N ENDOR data presented above show that there is no major shift of spin density from the O−O moiety to Fe.

While single-field ^{1}H ENDOR measurements are suggestive, a fuller understanding of the properties of the strongly coupled exchangeable proton associated with **5A** and **5B** requires the determination of the proton hyperfine coupling tensors, which requires the collection and analysis of full 2D, field/frequency datasets comprised of ENDOR spectra collected at numerous points across the EPR envelope. Such datasets have been collected for **5A** of the cryoreduced oxyD251N mutant and the **5B** species associated with the cryoreduced oxyP450 WT, D251N, and T252A mutants. Spectra collected in D_2O buffer confirm that the strongly coupled proton intensity is exchangeable; they further show the presence of other exchangeable proton(s), with maximum couplings of ~4 MHz. The data sets for **5A** of D251N mutant and the **5B** of WT enzyme are shown in Figure 8. As reflected in the figure, these experiments were constrained by an inability to collect spectra in a field range around g_2 that corresponds to most of the fields between roughly g_2 and g_3 of the cryoreduced oxyheme centers; these fields exhibit strong EPR signals from free radicals created by the irradiation, and these signals swamp those of the intermediates. Nonetheless, it is possible to trace enough of the field-dependent pattern for analysis.

Considering the 2D pattern for **5A** of D251N, Figure 8, upper, one sees a single ν_- peak in the g_1 spectrum that splits into two branches as the field is increased (g decreased); an additional feature that does *not* belong to the proton of interest also is indicated. The outer branch smoothly moves to a minimum frequency, corresponding to a maximum value of A, as the field is increased toward the vicinity of g_2; the inner branch increases in frequency (decreasing A) until it merges with the central, more intense signals. Spectra taken near g_3 again show a single ν_- peak. The maximum hyperfine coupling observed, $A = 14.4(2)$ MHz, corresponds to the maximum principle component of the hyperfine tensor. The g-value at which it occurs can be used to calculate the polar angle, $\theta \approx 40°$, between this tensor direction and the g_1 direction, which is shown above to be perpendicular to the heme plane. Numerous simulations of the field-dependent pattern led to a best fit which employed the hyperfine tensor given in Table 2. For completeness, the figure further notes (dashed line) a feature for an additional exchangeable proton whose coupling increases as g decreases from g_1 to a value of $A \approx 5$ MHz at ~g_2, then decreases. This might reflect a second stabilizing H-bond to the [O−O] moiety.

The spectra for the "hydroperoxo" proton that is associated with **5B** of oxyP450 WT, Figure 8, lower, generate a qualitatively similar 2D pattern, but one that is more compressed toward ν_H because the maximum hyperfine coupling is smaller, $A = 11.2(2)$ MHz. As a result, the outer branch is nicely visible, but the inner branch is lost almost immediately as the field is raised from g_1. The figure not only marks the features for this proton, but again points out an exchangeable proton with a maximum coupling of $A \approx 5$ MHz. The data are insufficient to permit an unconstrained fit to the 2D pattern, but given that the tensor for the strongly coupled proton of **5A** is nearly axial, we constrained that for the proton of **5B** to be axial and arrived

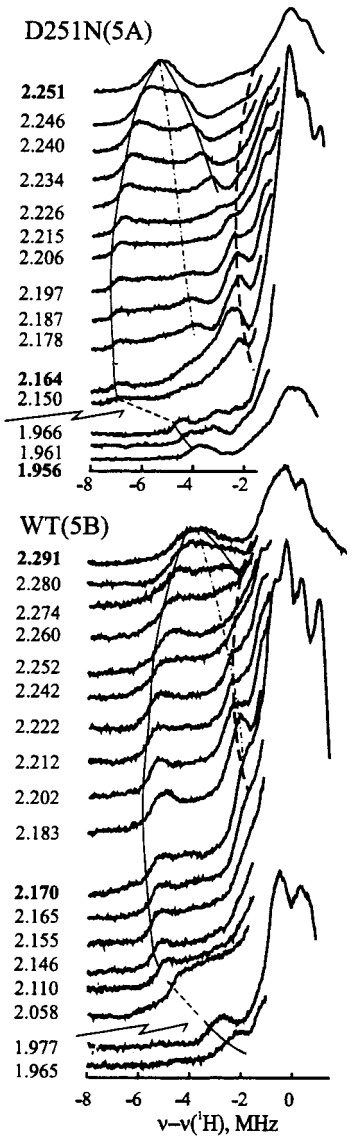

Figure 8. Orientation-selective, 2D field/frequency ^{1}H CW 35.2 GHz ENDOR patterns for cryoreduced oxyP450 intermediates **5A** (D251N) and **5B** (WT). *Conditions*: as in Figure 7.

Table 2. Hyperfine Tensors of Exchangeable Protons in Reduced OxyP450 Intermediates[a]

	5A				5B			
P_{450}	A_{max}	a, MHz	T, MHz	Θ (deg)	A_{max}	a (MHz)	T (MHz)	Θ (deg)
WT	-	-	-	-	11.2(2)	3.8(4)	3.7(3)	32(4)[c]
D251N	14.4(2)	8.0(5)	3.2(2)[b]	38(4)[b]	10.9(1)	3.4(7)	3.8(5)	33(4)[c]
T252A	-	-	-	-	11.5(3)	4.5(7)	3.6(5)	32(4)[c]

[a] The Table gives the maximum observed hyperfine interaction, A_{max}, as well as the isotropic coupling, a, and dipolar parameter, T, calculated under the assumption that the anisotropic contribution has the axial form, $[2T, -T, -T]$. The Euler angle, θ, corresponds to a rotation of the unique tensor direction, away from g_1 in the g_1−g_3 plane; ϕ corresponds to a rotation about g_1. [b] The best fit has $A = 14.2$, 5.1, 4.3 MHz, and T is reported as the average value; $\phi = 33(13)°$. [c] For these $0° < \phi < 33°$.

at the values given in Table 2. The Table also contains the tensors determined in the same fashion for the hydroperoxo proton in the **5B** state of the two mutants.

In each case, including both states **5A** and **5B**, the tensor of the strongly coupled proton has a dipolar component, $T \approx 3-4$ MHz and a polar angle of $\theta \approx 30-40°$ (Table 2). As the ^{14}N ENDOR results confirm that these paramagnetic centers all are low-spin ferrihemes, this constancy indicates that the proton in both the g_1-2.25 and 2.30 species lies at approximately the same location relative to the heme iron. Under a variety of reasonable assumptions, the value of T and the polar angle are compatible with predictions for a proton interacting with the distal oxygen atom of the $Fe-O_2$ fragment. The similarity in T for the g_1-2.25 and 2.3 species once again indicates that conversion of one to the other does not involve major shifts in spin (and charge) between O_2 and Fe. Nonetheless, the isotropic coupling to the proton drops ~2-fold in the g_1-2.3 species, indicative of a reduction in spin density on the remote O. This most likely reflects a large *percentage* drop in an already small spin density at the distal O.

Species 7A. The **g** tensor for the primary product-state, **7A**, Table 1, is essentially the same as that for the low-spin aquoferric form of the "model" enzyme, CPO.[37] Hence, we employed ^1H ENDOR to test the possibility that this intermediate, although containing product, actually has an aquo ferriheme in a nonequilibrium geometry. Figure 7 presents the ^1H ENDOR spectrum at g_1 of **7A** in cryoreduced oxyP450 D251N mutant annealed to 200 K. It shows the ν_- peak of a proton doublet with splitting of $A \approx 13$ MHz, almost exactly as seen at g_1 for the water protons in ls, aquoferri-P450 and CPO.[28,43] However, as shown in the figure, this proton signal is *not* lost in a sample that had been exchanged into D_2O buffer. We confirmed that the H/D exchange in this sample was complete through the observation (not shown) that the exchange completely abolished the exchangeable proton signals from **5A, B**, in this sample, as well as from the successor species **7B**, as discussed below. To confirm the lack of exchange in the g_1 spectra for **7A** (Figure 7), we compared the signals of **7A** in H and D buffers over a range of fields, Figure 9. Although the EPR spectrum of **7A** is superimposed on spectra of other species at fields higher than $g \approx 2.5$, Figure 4, at frequencies of interest (below ~−3 MHz) these other species only give signals from exchangeable protons. One can clearly observe the loss of some resonances from protons associated with these other species, but the signal from the strongly coupled proton(s) of **7A** is nonexchangeable, and can be followed over a range of fields. Because only a partial 2-D dataset is available for **7A**, analysis of Figure 9 to derive hyperfine tensor parameters is not warranted. However, in the Discussion we make further comments on the *magnitudes* of the hyperfine couplings, in particular the maximum coupling, $A_{max} \approx 13$ MHz.

Thus, the strongly coupled proton(s) of **7A** are *not* exchangeable in D_2O. But, what proton(s) are being observed? If **7A** contains an aquoferric heme generated during the hydroxylation reaction, the oxygen atom would have come from dioxygen but the protons would have been delivered during catalysis. Hence they would reflect the solvent composition, and appear "exchangeable", contrary to observation. The obvious assignment of **7A** is to a complex between the hydroxycamphor product and ferriheme, with the strongly coupled, nonexchangeable proton signals in Figures 7 and 9 arising from protons that originate on C5 of camphor. In the product, one of these protons remains attached to C5 and of course does not respond to solvent exchange. The other would become the hydroxyl H which thus appears to be *trapped in place* at 200 K.

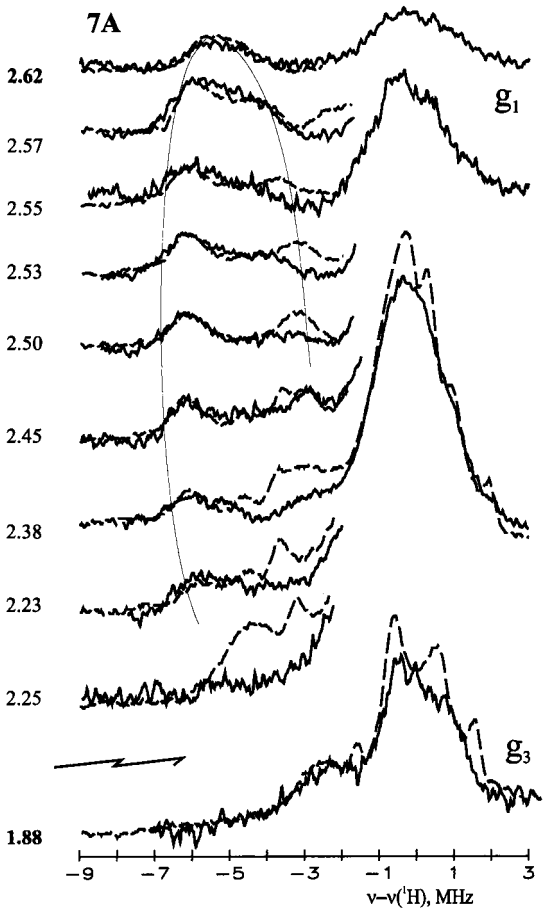

Figure 9. Orientation-selective, 2D field/frequency ^1H CW 35.2 GHz ENDOR patterns for intermediate **7A** (D251N). Dashed line, H_2O buffer; solid line, D_2O buffer. *Conditions*: as in Figure 7 except as follows: scan speed 1 MHz/s, 40 scans.

1-Adamantanol Complex. The only alternative assignment for the strongly coupled nonexchangeable protons of the g_1-2.62 species would be as the methylene protons of the proximal cysteinate. However, these protons have never been been seen to give large couplings in ENDOR studies of any other low-spin ferriheme form of either P450 or CPO.[28,42,43] Nonetheless, to help confirm the assignment of the nonexchangeable signals to substrate protons, we independently prepared the complex between ferric P450 and 1-adamantanol, the hydroxylation product of the alternate substrate, adamantane. The site of hydroxylation on adamantane is the C1 bridgehead carbon, and the product has no remaining C−H protons at the bridgehead. Thus, any strongly coupled, nonexchangeable protons detected in ENDOR spectra of this complex would necessarily be those of cysteine; note, by preparing the product complex "synthetically", the hydroxyl proton would reflect the solvent composition, and be exchangeable. Proton ENDOR studies of the adamantanol complex disclose an exchangeable proton with $A \approx 8$ MHz at g_1, which we assign to the hydroxyl hydrogen (not shown). However, the spectra do *not* exhibit a signal from a strongly coupled nonexchangeable proton. This result thus substantiates the assignment of **7A** as the primary product state following hydroxylation of camphor, with hydroxycamphor bound to iron in a nonequilibrium geometry.

Species 7, 7B. The annealing data for the D251N sample show that the initial product state **7A** converts to the g_1-2.5 intermediate, **7B**, which in turn converts to the g_1-2.48 equi-

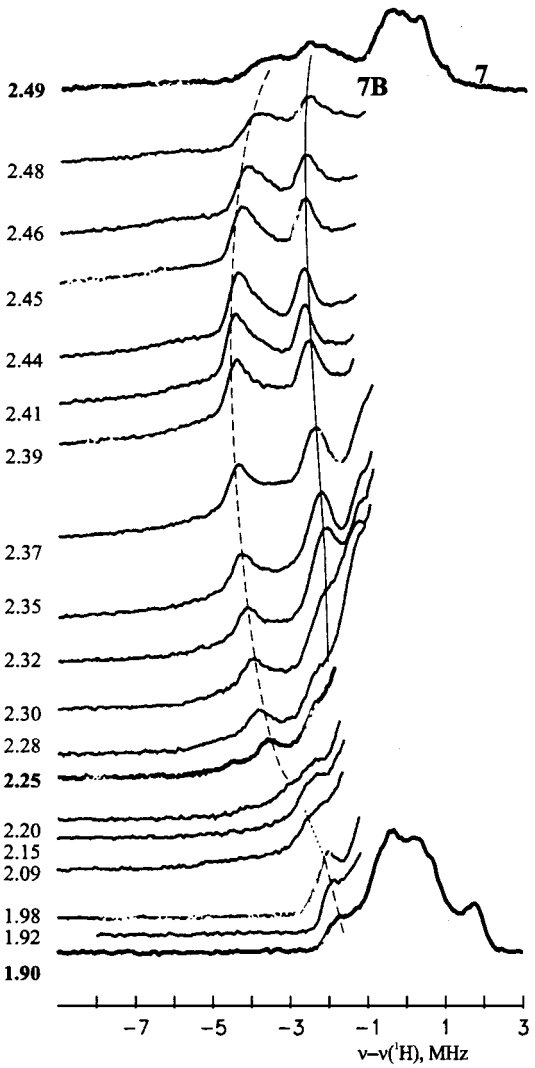

Figure 10. Orientation-selective, 2D field/frequency ^{1}H CW 35.2 GHz ENDOR patterns for the product complex **7** (D251N) prepared by addition of hydroxycamphor to resting state D251N (solid line), and for intermediate **7B** prepared by annealing of cryoreduced oxyD251N (gray line). *Conditions*: as in Figure 9.

librium product state, **7**. We discuss the equilibrium state first. We have generated **7** both by reaction of cryoreduced P450 WT and D251N, and also by addition of hydroxycamphor to the ferric resting state of these two variants, and find that the EPR and ENDOR spectra **7** are the same in the all cases. However, the large excess of product in the latter suppresses the aquoferriP450 species seen in Figure 2, and we present ENDOR data from the "synthetic" **7** prepared with the D251N mutant.

Figure 7 presents the ^{1}H ENDOR spectra collected at $g_1 = 2.48$ for **7** from P450 D251N in H_2O and D_2O buffers. The spectrum for H_2O buffer shows a pair of ν_- features corresponding to two protons with $A(g_1) \approx 2.5$ and 7 MHz. The spectrum with D_2O buffer shows that the larger coupling comes from an exchangeable proton, the smaller from one that is not exchangeable. We assign the nonexchangeable proton to H(C5) on hydroxycamphor bound to Fe, and assign the exchangeable one to the hydroxycamphor hydroxyl proton. (As with the adamantanol complex, by creating **7** synthetically the hydroxyl proton has been equilibrated with solvent, unlike the case of the trapped intermediate, **7A**.)

The 2-D field-frequency orientation-selective pattern for **7** is shown in Figure 10. For both protons, only the outer edge of the ENDOR pattern can be followed. For the nonexchangeable proton, a fit gave the hyperfine values of Table 3, with comparable isotropic and anisotropic contributions but rather large uncertainties in the relative contributions. The exhangeable proton can be described by an axial tensor dominated either by the isotropic or by the anisotropic part. Because the latter is expected for a hydroxyl proton,[43] we present the anisotropic analysis in Table 3; the isotropic analysis is included as a footnote to the table.

Table 3. Hyperfine Tensors of Strongly-Coupled Protons in the Equilibrium Hydroxycamphor-Ferri−P450−D251N Product Complex, **7**[a]

	7			
	A_{max} (MHz)	a (MHz)	T (MHz)	angles (deg)
nonexchangeable	5.7(2)	1.2(5)	2.2(2)	$\theta = 21(5)$ $\phi = 82(8)$
exchangeable	9.2(2)	0.7(4)	4.3(2)	$\theta = 22(5)$ $\phi = 44(12)$

[a] For definition of entries, see footnote *a* Table 2. [b] A second option, discussed in text, has $a = 5.6(4)$ and $T = 1.8(2)$, $\theta = 35(4)°$, $\phi = 82(8)°$.

Species **7B** clearly must be a product state that occurs along the reaction pathway by which the primary product state, **7A**, relaxes toward the equilibrium one, **7**. Clean spectra for **7B** are difficult to obtain because it is not formed quantitatively and overlaps with the EPR spectrum of the oxidized form, **2**. Nevertheless, reasonable data for **7B** could be obtained from a D251N sample annealed to 220 K. The g_1 proton ENDOR spectrum for **7B** shows a pair of ν_- features, the one with larger coupling being exchangeable, the other not (Figure 7), just as seen for species **7**, and the coupling constants are similar as well. Furthermore, Figure 10 shows that the field dependences of the two protons for **7B**, and in particular the maximum hyperfine couplings of $A_{max} \approx 9$ and 6 MHz for the exchangeable and nonexchangeable protons, respectively, correspond well to those of the two protons of **7**. We therefore assign these proton ENDOR signals for **7B** to the hydroxycamphor product, as for the two protons in **7**. As with **7A**, however, analysis of the proton hyperfine tensors for **7B** is not appropriate.

Thus, the primary product state relaxes to equilibrium as follows: **7A** → **7B** → **7**. In this process, the hydroxyl proton of hydroxycamphor in the primary product state, **7A**, is derived from substrate and is trapped in place during the formation of the **7** during annealing at ~200 K. Remarkably, the "doors" of this trap are opened by the minimal additional activation involved in annealing at 220 K to form **7B**. Note that this difference is not an artifact of annealing; the two nonequilibrium product states coexist for portions of the annealing process.

Discussion

Injection of the 'second' electron into oxyP450 (**4**) initiates catalysis and cryoreduction followed by controlled annealing has permitted a detailed scrutiny of subsequent steps in the catalytic cycle by EPR and ENDOR spectroscopies. This approach is fully validated by the demonstration that the cryoreduced enzyme hydroxylates substrate quantitatively and stereospecifically. These studies have characterized stages of the catalytic cycle between species **4** and **7** of Scheme 1, as summarized in the expanded portion of the cycle presented in Scheme 2.

The cryoreduction of the WT and mutant oxyP450s at 77 K, complemented by the 6 K cryoreduction experiment, indicates that the primary product formed by reduction of oxyP450 (**4**) is the g_1-2.25, "H-bonded, end-on peroxo" ferriheme form, denoted **5A**, which then converts to the hydroperoxo-ferriheme

Scheme 2

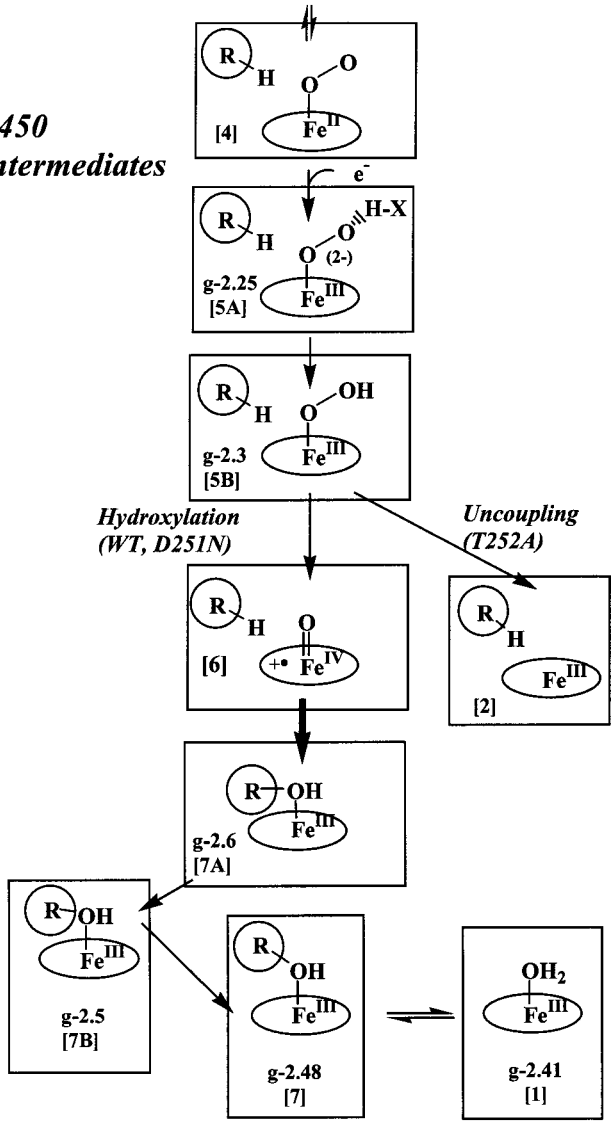

species **5B**. The kinetics of this conversion are significantly altered by mutations that influence proton delivery: T252A appears to convert completely at 77 K; WT converts incompletely at 77 K; D251N does not convert appreciably until temperatures above 130 K.

The **5B** intermediate for the "uncoupled" T252A mutant reverts to a ferriheme without product formation, presumably through addition of the second proton to the proximal oxygen of bound hydroperoxy and loss of H_2O_2 to the distal pocket. In contrast, annealing the WT and D251N **5B** to 200 K gives product. For the WT enzyme, little detail of this process is visible, but one does see a trace of a signal from the initial product state, **7A** ($g_1 \approx 2.62$), on the pathway to the g_1-2.48 EPR signal of the equilibrium product-bound state, **7**. Fortunately, the D251N mutation also appears to alter the kinetics of steps that follow the key catalytic one(s), so as to allow us to detect clearly a number of states not seen, or not seen well, for the WT enzyme. We suggest, however, that these nonetheless occur in the WT enzyme, but without ever building up sufficient concentration of intermediates for them to be EPR visible. Thus, we continue to build the sequence of catalytic steps in Scheme 2 through the observations from this mutant.

The ENDOR data shows that the P450 WT and D251N hydroperoxo-ferriheme intermediates, **5B**, convert without *detectable* intervening intermediates to the nonequilibrium, hydroxycamphor-bound g_1-2.62 state, **7A**. This subsequently relaxes to the equilbrium product-bound form, **7**, through the intermediate **7B** seen in EPR and ENDOR in the case of the D251N mutant. EPR and chemical quantitations indicate the reaction pathway that involves **5B** quantitatively yields 5-exo-hydroxycamphor.

Regarding the sequence of hydroxycamphor-bound product states, **7A** → **7B** → **7**, we note that the Fe−O distance in the equilibrium product state, **7**, is anomalously long, 2.67A, which is proposed to reflect a compromise between Fe−O bonding forces and unfavorable desolvation of the product OH group,[45] whereas the Fe−O distance immediately after the hydroxylation step should be shorter than 2 Å. We suggest that **7A** involves a more or less normal Fe−O distance, and that the heme pocket relaxes in two detectable steps to accommodate the longer bond at equilibrium. Note that the more normal bond length proposed to occur in **7A** would imply that the hyperfine coupling to the hydroxyl H should be roughly that found for the aquo-H of aquoferriP450. In fact, the signal at g_1 for **7A** has a similar maximum coupling constant and the field dependence, though only partial (Figure 6) is compatible as well.

What Is the Hydroxylating Species? The ENDOR data shows that the first detectable product state, **7A**, contains a hydroxycamphor bound to Fe^{3+}, and not a water-bound ferriheme state. Moreover, the proton whose bond to the C(5) carbon of substrate is broken during hydroxylation appears to be trapped in **7A** as the hydroxyl proton. These observations indicate that the reactive, hydroxylating species in P450cam is indeed the high-valent, intermediate **6**, Scheme 1, and that the reaction does not occur by direct electrophilic attack of the remote oxygen of hydroperoxyferri intermediate, **5B**, an alternate pathway that may occur in other monooxygenases.[46,47]As illustrated in Scheme 3, in a hydroxylation that involves formation of and attack by the oxyferryl moiety of **6**, the water produced upon splitting the hydroperoxo moiety of **5B** is lost prior to hydroxylation, and the primary product state would contain hydroxycamphor bound to the ferriheme through its hydroxyl, with one of the two H(C5) of the reactant camphor as the hydroxyl proton. This is completely consistent with our experiments. In contrast, as shown in Scheme 3, direct hydroxylation by the remote oxygen atom of a hydroperoxo-ferriheme would leave a water/hydroxide bound to Fe, contrary to observation, and this water would contain protons that derive from solvent, not substrate. To reconcile the ENDOR data with attack by Fe-bound hydroperoxo would require the implausible postulate of an unobserved state prior to **7A** in which water/hydroxide is bound to the ferriheme, and the assumption that *at the temperature where hydroxylation is observed*, ~200 K, this water/hydroxide "jumps out of the way" of the hydroxycamphor which replaces it as a heme ligand.

Effects of Mutations. These results clearly speak to the role of T252 and D251 in ways previous studies could not. As discussed above in the Introduction, it has been proposed that these residues are involved in proton delivery during catalysis. The recent low-temperature crystal structure of the P450cam−O_2−camphor ternary complex, **4**, by Schlichting et al.[17]showed that binding of dioxygen to ferrous heme is accompanied by

(45) Li, H.; Narasimhulu, S.; Havran, L. M.; Winkler, J. D.; Poulos, T. L. *J. Am. Chem. Soc.* **1995**, *117*, 6297−6299.
(46) Newcomb, M.; Shen, R.; Choi, S.-Y.; Toy, P. H.; Hollenberg, P. F.; Vaz, A. D. N.; Coon, M. J. *J. Am. Chem. Soc.* **2000**, *122*, 2677−2686.
(47) Pratt, J. M.; Ridd, T. I.; King, L. J. *J. Chem. Soc., Chem. Commun.* **1995**, 2297−2298.

Scheme 3

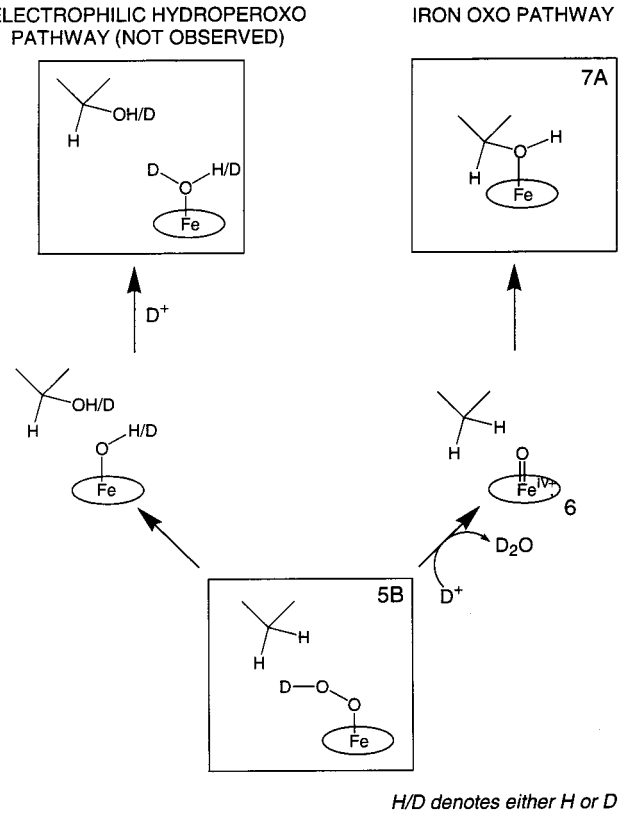

an intriguing backbone rearrangement involving D251, movement of camphor, and the appearance of two additional water molecules in the heme pocket close to both the dioxygen ligand and hydroxyl group of T252. The side chain of T252, but not that of D251, is involved in a distal-pocket hydrogen-bonding network that stabilizes bound O_2, and likely is involved in proton delivery.

Our results show that in WT enzyme the primary product formed upon reduction of **4**, namely **5A**, converts to the hydroperoxy intermediate **5B** at very low temperatures, with most of the conversion by 77 K and the remainder by ~160 K. This step is not hindered by the T252A mutation; it may even be facilitated in that there appears to little or no contribution of the precursor, **5A,** to EPR spectra taken from samples not annealed above 77 K. It is noticeably hindered by the D251N mutation, for which conversion of **5A** to **5B** begin only at ~140 K; interestingly, however, for D251N, conversion is completed by ~160 K, not substantially different than the others. Of key importance, within the precision of these measurements, the reaction of **5B** during 1 min annealing steps occurs over a range of temperatures of roughly ~190−210 K in *all three cases*, the two which form product, WT and D251N, and the one which is decoupled, T252A.

Our observations for the T252A mutant thus are completely consistent with the idea that it plays a key role in the delivery of the second proton of catalysis, in that the disruption of catalysis caused by this mutation occurs after the first proton has been delivered, to form **5B**. Likewise, these results support the idea that the D251N mutation influences catalysis during the steps involving delivery of the first proton: once **5B** is formed in the D251N mutant, it goes on to form product quantitatively at low temperatures. The D251N mutation, however, has the further effect of influencing steps after the hydroxylation reaction, even as it influences the **5A** → **5B** precursor process. Thus, the initial product state, **7A**, barely builds up to detectable levels at ~210 K in WT enzyme, for which the equilibrium product state accumulates and dominates spectra by ~220 K, and **7B** is not seen. However, for D251N, **7A** builds up appreciably, to a maximum at ~215 K, and an additional product state (**7B** ($g_1 = 2.5$)) is seen as **7A** relaxes to the equilibrium form, **7**. The conversion, **7A** → **7B** introduces an exchangeable proton into the ENDOR spectra, indicating that the hydroxylic proton derived from H(C5) of camphor now is able to exchange with protons ultimately derived from the solvent.

Observation of High-Valence Intermediate 6? Our data implicate the high-valent intermediate **6** as the hydroxylating intermediate in P450 cam, in support of the "standard" model for hydroxylation in this enzyme.[48,49] However, our systematic annealing experiments have yielded no spectroscopic evidence for **6**, suggesting that it is too reactive to build up to observable levels, but rather reacts promptly to form product even at ~200 K.

Has **6**, nonetheless, been detected in other ways? Two spectroscopic reports are significant in this context. In one, a transient optical signal was observed in stopped-flow experiments in which the camphor complex of ferriP450 reacts with *m*-chloroperbenzoic acid.[16] This signal was considered as possibly arising from **6**, but the assignment has not yet been corroborated. Recently, substrate-free ferriP450 (**1**) was reacted with peroxy acetic acid, freeze-quenched, and intermediates examined by Mossbauer and EPR spectroscopies.[38] A species was identified that contains an Fe(IV) ($S = 1$), presumably oxyferryl, along with an uncoupled radical that is assigned to tyrosyl. As noted in that report, this species is not a Compound I, but rather a Compound II with a noncoupled radical, and thus represents a side-reaction in which one of the oxidizing equivalents from the peroxy acetic acid has migrated to an amino acid residue. Such degradative processes also occur, for example, in the reaction of hydrogen peroxide with myoglobin.[50]

Schlichting et al. not only presented the X-ray structure of **4**, but also of intermediates arising after radiolytic reduction of the crystal at cryogenic temperature.[17] They found that the structure of oxyP450 exposed to X-ray irradiation at cryogenic but undefined temperature reveals a species with electron density centered above the heme iron at a distance of ~1.65 A. The authors suggested that this species might be **6**, but they could not exclude the possibility that it involved an aquoferriheme. The result also would be consistent with the Compound II/tyrosyl radical species reported subsequently.[38] However, in these experiments hydroxycamphor was shown to be formed after thawing the irradiated crystals.

The crystallographic result also can be discussed in the context of the EPR/ENDOR data. Recall that in our annealing experiments **5B** in the WT enzyme converts to the product state **7** over a narrow temperature range: **5B** does not react during 1 min at 180 K, but reacts completely during 1 min annealing at 195−200 K. However, the temperature of a sample during cryoreduction in a synchrotron beam is *not* well controlled, which makes it appear improbable that the crystal in the X-ray beam could have fortuitously been raised briefly to within a narrow temperature range such that **6** builds up appreciably without reacting, then promptly cooled to stabilize **6** before it reacts to form product, and that this could occur in multiple

(48) Groves, J. T.; Han, Y.-z. In *Cytochrome P450*, 2nd ed.; Ortiz de Montellano, P. R., Ed.; Plenum Press: New York, 1995; pp 3−48.
(49) Ortiz de Montellano, P. R. In *Cytochrome P450*, 2nd ed.; Ortiz de Montellano, P. R., Ed.; Plenum Press: New York, 1995; pp 245−304.
(50) Gunther, M. R.; Sturgeon, B. E.; Mason, R. P. *Free Radical Biol. Med.* **2000**, *28*, 709−719.

samples. Thus, our data appears to imply that the species characterized by diffraction is not catalytically competent. This issue needs further investigation, because one must consider the possibility that the enzyme frozen in solution and frozen in a crystal reacts in different ways, with **6** building up in crystal but not solution.

Summary

We have employed γ-irradiation at cryogenic temperatures (77 K but also ~6 K) of the ternary complexes of camphor, dioxygen, and ferro-cytochrome P450cam to inject the "second" electron of the catalytic process, allowing us to detect and examine stages in catalysis between species **4** and **7** of Scheme 1. We have used EPR and ENDOR spectroscopies to study the primary intermediate as well as subsequent states created by annealing reduced oxyP450, both the WT enzyme and the D251N and T252A mutants, at progressively higher temperatures. (i) The primary product formed by reduction of oxyP450 4 is the end-on, "H-bonded peroxo" intermediate **5A**. (ii) This converts even at cryogenic temperatures to the hydroperoxo-ferriheme species, **5B**, in a step that is sensitive to these mutations.Yields of **5B** are as high as 40%. (iii) In WT and D251N P450s, brief annealing in a narrow temperature range around 200 K causes **5B** to convert to a product state, **7A**, in which the product 5-exo-hydroxycamphor is coordinated to the ferriheme in a nonequilibrium configuration. Chemical and EPR quantitations indicate the reaction pathway involving **5B** yields 5-exo-hydroxycamphor quantitatively. Analogous (but less extensive) results are seen for the alternate substrate, adamantane. (iv) Although the T252A mutation does not interfere with the formation of **5B**, the cryoreduced oxyT252A does not yield product, which suggests that **5B** is a key intermediate at or near the branch-point that leads either to product formation or to nonproductive "uncoupling" and H_2O_2 production. The D251N mutation appears to perturb multiple stages in the cycle. (v) There is no spectroscopic evidence for the buildup of a high-valence oxyferryl/porphyrin π-cation radical intermediate, **6**. However, ENDOR spectroscopy of **7A** in H_2O and D_2O buffers shows that **7A** contains hydroxycamphor, not water, bound to Fe^{3+}, and that the proton removed from the C(5) carbon of substrate during hydroxylation is trapped as the hydroxyl proton. This demonstrates that hydroxylation in fact occurs by the formation and reaction of **6**. (vi) Annealing at $\geq$220 K converts the initial product state **7A** to the equilibrium product state **7**, with the transition occurring via a second nonequilibrium product state, **7B**, in the D251N mutant; in states **7B** and **7** the hydroxycamphor hydroxyl proton no longer is trapped. (vii) The present report does not provide support for the possibility that an intermediate state observed recently by crystallographic methods [17] actually corresponds to the catalytically competent intermediate, **6**.

Acknowledgment. We acknowledge grants from the National Institutes of Health to S.G.S. (GM33775 and GM31756) and B.M.H. (HL13531). Work at Argonne was performed under the auspices of the Office of Basic Energy Sciences, Division of Chemical Science, US-DOE under Contract Number W-31-109-ENG-38.

Supporting Information Available: Figures S1−S3 in Supporting Information present, respectively, the spectra from every annealing step for the T252A, WT, and D251N P450s in H_2O buffer; Figure S4 presents the data for the last in D_2O buffer (PDF). This material is available free of charge via the Internet at http://pubs.acs.org.

JA003583L